Elucidating the effect of spin crossover materials on graphene sensing devices

Krishna Maity, Jean-François Dayen, Marlène Palluel, Nathalie Daro, Guillaume Chastanet, Bohdan Kundys, Bernard Doudin

Elucidating the effect of spin crossover materials on graphene sensing devices

Krishna Maity[1*], Jean-François Dayen[1], Marlène Palluel[2], Nathalie Daro[2], Guillaume Chastanet[2], Bohdan Kundys[1], Bernard Doudin[1*]

[1]Université de Strasbourg, CNRS IPCMS, 23 Rue du Loess, Strasbourg, F-33608, France

[2]Université de Bordeaux, CNRS, Bordeaux INP, ICMCB, 87 avenue du Dr A. Schweitzer, Pessac, F-33608, France

*Corresponding authors: krishna.maity@ipcms.unistra.fr; bernard.doudin@ipcms.unistra.fr

Graphene films are used to detect the presence and transition of spin crossover nanoparticles aggregates. Experiments performed far from the graphene neutrality point, combining impedance spectroscopy and Hall measurements, provide better insight into the mechanism for the change of impedance of the graphene layer in proximity with different states of the molecular structure. We observe that the change of spin state shifts the graphene Fermi level and its intrinsic resistance, with resulting positive insight into using this type of hybrid device for fast molecular electronics purposes.

Spin crossover (SCO) materials are well-documented model of bistable molecular system. Their robust spin state transition behavior triggered by multiple external stimuli like temperature, pressure, light and electric field make them promising for numerous applications [1–3]. Their change of magnetic properties, optical absorption, structural and dielectric properties make them promising candidates in the application of data storage, nanotechnology[4], optoelectronic devices, and sensors[5]. However, like most molecular materials, they are insulating in nature, limiting their integration into electronic devices[6]. On the other hand, graphene is a highly conducting material, highly sensitive to its environment[7–9]. Pioneering the combination of these two unique materials, Dugay et al. investigated self-assembled layers of SCO nanoparticles on top of graphene transistor devices and observed how their hysteretic temperature change of conductance related to the spin transitions of the SCO[10]. They proposed that it resulted from phonon modes coupling to the charge carrier of graphene that enhanced scattering, with a resulting change of carrier's mobility. The charge transport of graphene/SCO devices have also been studied on a model SCO single crystal, separated from graphene by a thin polymer spacer. Here the authors found experimental and theoretical arguments molecular phase-dependent electrostatic coupling between the two materials.[11]. The electrical transductions of both thermal and light induced spin transition (LIESST) at low temperature have been demonstrated on graphene sensor interfaced with sublimated SCO thin film, and interpreted as shift of the Fermi energy level of the graphene layer upon the switching of the molecular state [12]. A model of strain-induced change of

graphene conductivity has also been recently put forward to explain the influence of SCO thin films change of phase.[13] However, most reported graphene transistor devices were studied near the neutrality point of the graphene, where it is most difficult to untangle changes of mobility and number of carriers (indicative of a change of Fermi level). There is therefore a need of clarifying the issue, check if the mechanism depends on the type of SCO materials used: nanoparticles, single crystal, or thin films, and test if any proposed mechanisms defined for such ordered SCO materials can be extended to a more disordered and discontinuous material. This could then guide design constraints for large scale integration of SCO systems for device applications as well as validate the robustness of the proposed strategy for making graphene-molecular materials hybrids.

Better understanding can also be put to question possible higher frequency operation of hybrid graphene devices. An important bottleneck in molecular electronics applications is their considered limited speed capabilities when compared to standard semiconductor device technologies. Even though a few reports of fast switching molecular devices can be found in the literature[14,15], their integration into scalable circuitry remains elusive. The switching of SCO materials can occur at the ns time scale when their size is reduced down to the nanoscale, at which one can still take advantage of the molecules collective behavior.[16] This makes nanoparticles size and shape of utmost importance if operation speed relevance for memory device applications is mandatory. The well-established capability of graphene for fast electronics[17] makes hybrid molecular nanoparticles-graphene devices possible contenders for RF molecular electronics applications.

Impedance spectroscopy (IS) is a widely used technique of choice to better understand relaxation of charge carriers and charge transfer at interfaces in materials ranging from bulk to nanoscale. The interfacial behaviour in graphene-silicon[18], interlayer charge transfer in dielectric with graphene[19–21] and the effect of interface modification[22] between graphene and SiO_2 were explored with IS. In this article, we propose to get better insight into the coupling mechanism of SCO particles drop-casted on graphene devices using IS data. This will also go beyond the reported data, currently limited to DC measurements in the literature, and provide insight into broader band electronics device capabilities.

CVD grown single layer graphene on SiO_2/Si substrate was bought from Graphenea. Before patterning, the devices were kept at 250° C for 12 h inside a glovebox to remove moisture and residue in the CVD grown and transferred graphene. Two types of devices were then patterned and connected with Au electrodes using optical lithography and Ar etching.

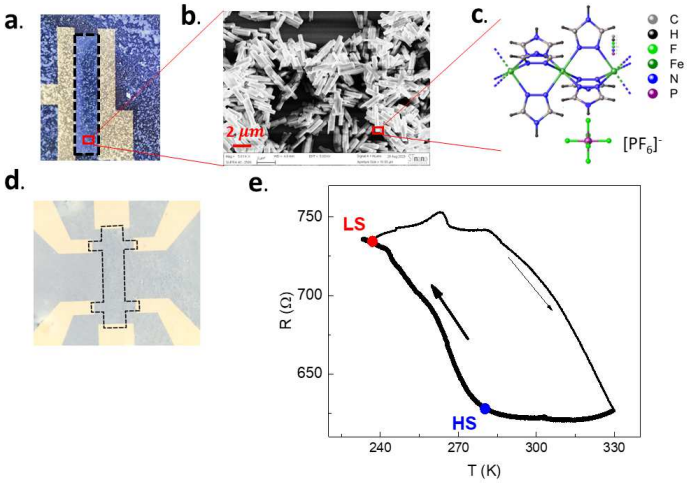

Fig. 1: Graphene devices with drop casted SCO material used for measurements. (a) two-probes design for impedance spectroscopy measurements; (b) SEM picture of the SCO coverage made of ensembles of elongated particles; (c) sketch of the $Fe(Htrz)_2trz^+$ molecule (with $(PF_6)^-$ counterions) with dashed lines indicating the intermolecular binding creating polymer-like ensembles; (d) four-probes design for longitudinal and transverse (Hall) resistance measurements; the patterned graphene area is emphasized by the dashed lines area, of size of 1.8 mm X 0.5 mm and 1.4 mm X 0.3 mm respectively; (e) temperature hysteresis of the Gr/SCO device resistance.

SCO $[Fe(Htrz)_2trz)^+(PF_6)^-]$ particles were synthesized by following a procedure previously reported[23]. They were then dispersed in ethyl alcohol by ultrasonication for 5 minutes and drop casted on the graphene device. The SEM image in Figure 1 (b) shows elongated particles of typical 3000 nm by 500 nm size, strongly agglomerated, defining the graphene-nanoparticles hybrid, further denominated Gr/SCO. These devices were then heated for 12 hours at 80° C in vacuum to limit moisture and solvent residues. Figure 1b illustrates the typical coverage of all samples studied, that we estimate in the 50-70% range. Adding particles was found to have little influence on the sample properties, not exceeding reproducibility in measurements.

Two electrodes' devices for impedance spectroscopy studies (1800 μm×500 μm, Fig. 1(a)) and four electrodes Hall-bar devices (1400 μm× 300 μm, Fig. 1(d)) were defined by laser lithography and 10 nm/40 nm Ti/Au interconnects lift-off over the etched graphene areas. IS measurements were performed by lock-in technique in a frequency range from 100 Hz to 5 MHz in a variable temperature probe station under low pressure N_2 atmosphere, and Hall measurements performed in a Quantum Design PPMS system under low pressure He atmosphere.

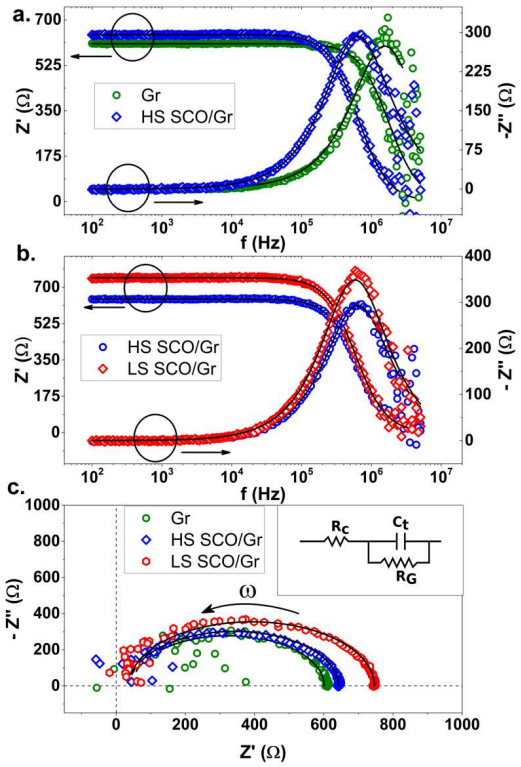

Fig. 2. Variation of real part Z' and imaginary part -Z'' with frequency: (a) comparison between bare graphene and Gr/SCO at 280 K (HS); (b) comparison between two different spin states of SCO/Gr, measured at 240 K and 280K (points in Fig. 1e); (c) Nyquist Plots (-Z'' vs Z') fitted with the circuit model in the insert.

The Gr/SCO device exhibits resistance versus temperature value following the SCO spin state change of phase, with hysteretic variation with temperature (Fig. 1e) indicative of the collective behavior reported for nanoparticles ensembles. This is in strong contrast with the resistance of pristine CVD graphene varying little and monotonically in the measured temperature range[12]. The Gr/SCO resistance increases significantly when cooling and SCO particles changing their spin state from HS to LS with a transition temperature of $T_{1/2}^{\downarrow}$ = 256 K that matches the one measured by magnetometry on the powder initial sample. [10–12] When heating up, the expected hysteresis of the SCO transition is observed, with a measured $T_{1/2}^{\uparrow}$ = 306 K, significantly larger than the one found by magnetometry (278 K) and in our own previous experiments.[24]

While the cooling curve transition was reproducible (on more than 10 samples tested) with a variation of resistance upon transition in the 5 to 20% range on 80% of the samples, the frequently observed sample resistance drifts under temperature sweeps, increasing when increasing the temperature, made the heating curve less reproducible. Electric transport measurements are therefore limited to the cooling part of the hysteresis, at 280 K where most molecules are expected to be in the HS state and at 240 K where most molecules are expected in the LS state. IS data is presented in Fig. 2, where we compare the spectra of bare graphene (at 280K, with little temperature variation) and Gr/SCO at 240K and 280 K in the expected LS and HS majority states (Fig. 2 a, b). Measurements are performed at zero gate bias, with gate Si substrate and source electrode grounded, to ensure long term stability of the impedance, key for reliable data acquisition. At such gate value, graphene is p-doped, quite far from its Dirac point, in agreement with our previous findings on similar samples with smaller particles,[24] as well as test measurements of full transfer curves (SI, Fig. S1). The real part of the impedance ($Z^{'}$), or resistive part of the device, remains approximately constant in the low frequency range and decreases with increasing frequency. A Nyquist plot (Fig. 2c) shows a typical semi-circle aspect of a simple equivalent circuit, made of a series resistor in series with two parallel resistor and capacitor (inset Fig. 2c). The setup leads capacitance due to cabling and micromanipulators tips was previously measured using calibrated sample resistors and estimated at 170 pF, a value we subtracted from the fitted total capacitance of the circuit in the 500 pF range. We therefore suppose that the sample resistance R_G in Fig. 2c relates to the intrinsic conductivity of the graphene film and that the total capacitance C_t sums the several surrounding capacitances of the graphene film. The quantum capacitance of graphene, and the capacitance of the SCO over-layer cannot exceed the aF range, more than four orders of magnitude lower than the fitted values. C_t therefore corresponds to the SiO_x substrate capacitance, separating the circuit from the conductive Si/bottom ground electrode in this bottom gate FET device configuration.

Table 1: Table for fitted parameters contact resistance (R_c), graphene channel resistance (R_G), total capacitance (C_t), Hall coefficient (R_H), deduced charge carrier density, measured longitudinal resistance in Hall-bar device (R_L) and deduced Hall mobility (μ_H) in the graphene channel.

	R_c (Ω)	R_G (Ω)	C_t (nF/cm^2)	Trapping charge density (cm^{-2})	R_H (Ω/T) ±1%	Carrier density (cm^{-2}) ±1%	R_L (Ω) ± 1%	μ_H $(cm^2/V.s)$ ±2%
Graphene	46±7	550 ± 30	35 ± 5	(2.2±0.3) ×10^{10}	61	10.2×10^{12}	3140	194
Gr/SCO at 280 K	39±6	600 ± 20	49 ±3	(3.0±0.2) ×10^{10}	192	3.3×10^{12}	4013	478
Gr/SCO at 240 K	37±5	710±23	52±3	(3.3±0.2) ×10^{10}	212	2.9×10^{12}	4411	480

Resulting fitted values are tabulated in Table 1. The contact resistance R_c is almost constant and doesn't vary significantly compared to the graphene channel in the range of measured temperature, as expected. The resistance of graphene R_G increases when covered by SCO material, further increasing when cooling down and going from the HS to the LS phase of SCO. Note the errors indicated in Table 1 result from the fitting procedure and are overestimated for R_G as measurements are performed in the low frequency range only, as illustrated in the data below 10 kHz in Fig. 2a and 2b. The capacitance of our CVD grown graphene device (of the order of several tens of nF/cm^2), on-par with the literature on CVD graphene over SiO_2 substrates, [22] originates from trap sites at the interface of silicon oxide and graphene. Within 4-8 nm, impurity and defects create trap sites which are most commonly positively charged (N^+_D)[25], capable of electron trapping ($N^+_D + e^- \rightarrow N_D$) and release ($N_D \rightarrow N^+_D + e^-$) by Schottky emission[26]. Graphene becomes hole doped due to the trapping of electrons by these trap sites[27], as previously measured on similar samples.[24] One can model the total Gr/Si capacitance as the sum of the interface capacitance, here mostly due to the trap sites, with the bulk 300 nm thick SiO_2 substrate dielectric capacitor. The latter is however much larger than the interface capacitor, which will then dominate the fitted value. The number of trap charges can be then estimated as $n \approx V_{SD} C_{interface}/e$ (V_{SD}= 0.1 V). Impedance data therefore indicates a change of graphene intrinsic conductivity combined with a change of the number of trap sites when adding SCO particles and modifying their spin state. This trend was observed on all measurements (on four samples), with however significant variations in the values and their relative change. Another example is given in the SI (Fig. S2).

Further insight is gained by performing Hall measurement on similar material patterned with a Hall bar geometry, to better pinpoint the origin of the changes of conductance of the graphene. While IS was performed on several samples, Hall data was measured on one. We chose a device with stable enough resistance at 280 K under magnetic field sweeps experiments and compare the IS data in Fig. 2 from a sample patterned and covered with SCO particles in the same lithography and baking batches. The longitudinal Hall resistance value R_L follows the same trend as R_G (Table 1) and confirm the reproducibility of the trend of the IS analysis. The Hall resistance R_H varies linearly with magnetic field and is shown in Fig. 3. The sign of the Hall coefficient confirms that holes are the majority charge carrier in graphene[28]. The Hall coefficient, which is directly related to the charge carrier density ($R_H = -\frac{1}{ne}$; n is charge carrier density and e is electron charge 1.6×10^{-19} Coulomb), increases significantly in the device after deposition of the SCO particles and further increases by the changing of spin states, with the carrier densities listed in Table 1. The Hall mobility is calculated using the formula $\mu_H = R_H/R_L$. Table 1 shows how mobility increases remarkably when covering graphene with SCO particles, confirming the IS results. However, there is no significant change of mobility under SCO transition. This is consistent with our previously

reported results with field effect transistor measurements.[24] Note that the Hall measurements provide a more reliable insight into mobility values, as they should not be influenced by trapping-untrapping of interfacial states, possibly sensitive to applied electric fields.

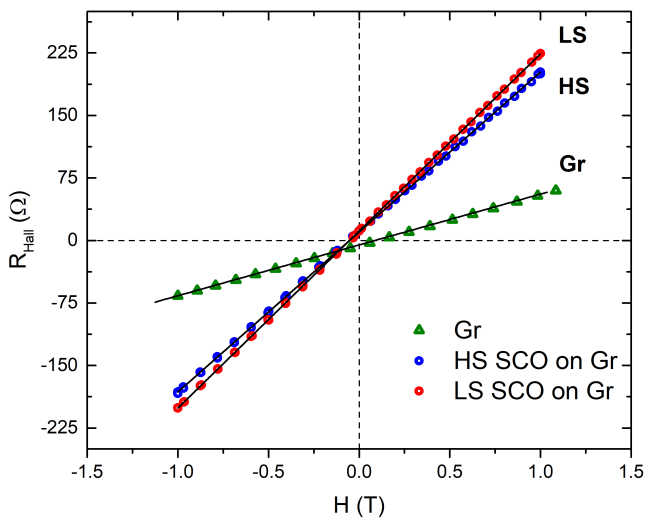

Fig. 3: Variation of Hall resistance with magnetic field comparing the initial graphene FET with the same device with SCO nanoparticles in their two different spin states, measured at temperatures shown in Fig. 1e and used for the data of Fig. 2.

The change of graphene properties under SCO transition values are consistent with previously reported data on similar graphene devices[12,29,30]. The SCO particles have intrinsic electrical polarization due to either the molecules electrical dipoles or to their combinations with counterions co-crystallized in the material[11,31]. This electrostatic gating de-trap electrons from the trap sites with a resulting increased number of positively charged trap sites, and hence increased total capacitance of the device. When adding SCO particles, a change of around 70 % of number of graphene charge carriers is mirrored by the same order of magnitude of change of trap sites, around 50%. This trend is confirmed by the same relative change of around 10% when switching the SCO state from HS to LS. The emerging picture is that SCO material changes the population of (charged) trap sites, increasing when releasing e^-, which in turn diminish the graphene layer doping. We recall here that we are investigating an intrinsically highly doped graphene material, where the

graphene carrier's mobility is expected to vary little with the number of carriers. As adding SCO particles impacts by 10-20% the graphene resistance (R_G or R_L), a very significant increase of mobility, directly resulting from Hall measurements, is observed. This is in contrast with most studies of doping effect of molecular adsorbates on graphene [32,33], where results systematically report a decreasing mobility when adding molecules on graphene.

The observed change of graphene properties under the transition of the SCO state is however quite different in origin. Here, the 10-20% change in graphene resistance comes from a similar change of carrier densities, without noticeable change in the measured Hall mobility. Even though μ_H is sensitive to the presence of SCO, it is invariant under the molecular phase transition. Therefore, the graphene detects the occurrence of the spin transition through a simple shift of Fermi energy. The origin is again most probably electrostatics, where we expect that the structural change experienced by the SCO material modifies its electronics clouds configuration, especially at its surface, and therefore changes the number of carriers in graphene through the substrate trapping sites. We do not foresee any strain contribution, as the SCO coverage of the graphene is discontinuous and partial, and large strain values would be needed to significantly modify the graphene conductivity.

In summary, we found that adding SCO nanomaterial to graphene impacts the density of carriers, mostly through the de-trapping of the silicon oxide substrate states. Surface charges of the SCO particles screen the local electrostatics, which can possibly explain the increase of mobility when adding the particles, unusual for molecular adsorption on graphene. The observed changes of density of carriers and intrinsic graphene device resistance confirms the electrostatics nature of the detection of the SCO presence as well as its phase. Our results indicate that such a mechanism can apply to disordered adsorbed film, with a large size dispersion, without a need of well-organized single crystal, thin film, or self-assembled layer of identical small particles. Impedance measurements confirm the intrinsic resistive nature of the graphene hybrid device. The cut-off frequency is driven by the substrate capacitance, limited to around 500 kHz for the large-scale mm^2 area devices studied here (reaching 1 MHz for the sample in the SI, Table S1). Such limitation originates from intrinsic properties of the silicon oxide and graphene. For μm^2 sized devices, smaller by 5-6 orders of magnitude, the capacitance should scale down similarly. One can therefore expect the cutoff frequency to increase by orders of magnitude. Gr/SCO devices involving adsorbed nanoparticles material have therefore high-frequency electronics capabilities that should match those of CVD graphene transferred on SiO_2. Even though such graphene substrates are not usually chosen for FET highest frequency studies, we remind here that the main approach for isothermal switching for SCO materials is the use of light, making then the top SOC film a 'top gating' material, best suited for fast FET switch operation. Moreover, this SOC material offers room temperature operability by means of light-triggered switching

operation[24]. The far-fetched GHz operation speed, matching the expected optically induced transition time scale,[16,34] might therefore be possible, under the hypothesis that the particles surface charges configuration will follow their light-triggered switching. While there are still unknowns in the 3-4 orders of magnitude needed to reach GHz operation, we consider that graphene sensors of SCO nanoparticles are ideally suited for this goal, with the perspective of easy to process ideal and robust contenders for fast molecular electronics devices.

Supplementary Informations

Complementary information is provided: trandfer curve of a two-terminals device (Fig. S1), another example of IS data, showing a 1 MHz cutoff, (Fig. S2), with table summarizing the equivalent circuit values (Table S1) that compare to Table 1.

Author Contributions

K.M. and B.D. initially designed the experiment, then helped by G.C, J.D. and B.K. K.M: performed measurements, with the help of J.D. and B.K. M.P., N.D. and J.C. synthesized the material and use protocols. K.M. and B.D. wrote the manuscript, seconded by all coauthors.

Acknowledgements

We thank Fabien Chevrier and the staff of the STnano nanofabrication facility for daily support and J. Robert for PPMS measurements. This project has received funding from the Agence Nationale de la Recherche (HEROES ANR-17-CE09-0010-01) and the European Union's Horizon 2020 research and innovation programme under the Marie Skłodowska-Curie grant agreement MaMi No. 766007 and QUSTEC No. 847471, the Interdisciplinary Thematic Institute QMat, as part of the ITI 2021 2028 program of the University of Strasbourg, CNRS and Inserm, was supported by IdEx Unistra (ANR 10 IDEX 0002), and by SFRI STRAT'US project (ANR 20 SFRI 0012) and EUR QMAT ANR-17-EURE-0024 under the framework of the French Investments for the Future Program. B.D. aknowledge the support of the Institut Universitaire de France.

Data Availability

Data is available upon request to the corresponding authors.

References

[1] P. Gütlich, and H.A. Goodwin, editors , *Spin Crossover in Transition Metal Compounds I-III* (Berlin ; New York, 2004).
[2] M.A. Halcrow, editor , *Spin-Crossover Materials: Properties and Applications* (Chichester, West Sussex, United Kingdom, 2013).
[3] G. Molnár, S. Rat, L. Salmon, W. Nicolazzi, and A. Bousseksou, "Spin Crossover Nanomaterials: From Fundamental Concepts to Devices," Adv. Mater. **30**(5), 1703862 (2018).
[4] C. Lefter, V. Davesne, L. Salmon, G. Molnár, P. Demont, A. Rotaru, and A. Bousseksou, "Charge Transport and Electrical Properties of Spin Crossover Materials: Towards Nanoelectronic and Spintronic Devices," Magnetochemistry **2**(1), 18 (2016).
[5] E. Resines-Urien, E. Fernandez-Bartolome, A. Martinez-Martinez, A. Gamonal, L. Piñeiro-López, and J.S. Costa, "Vapochromic effect in switchable molecular-based spin crossover compounds," Chem. Soc. Rev. **52**(2), 705–727 (2023).
[6] F. Prins, M. Monrabal-Capilla, E.A. Osorio, E. Coronado, and H.S.J. van der Zant, "Room-Temperature Electrical Addressing of a Bistable Spin-Crossover Molecular System," Adv. Mater. **23**(13), 1545–1549 (2011).
[7] T.-H. Han, H. Kim, S.-J. Kwon, and T.-W. Lee, "Graphene-based flexible electronic devices," Mater. Sci. Eng. R Rep. **118**, 1–43 (2017).
[8] Y. Zhang, R. Ma, X.V. Zhen, Y.C. Kudva, P. Bühlmann, and S.J. Koester, "Capacitive Sensing of Glucose in Electrolytes Using Graphene Quantum Capacitance Varactors," ACS Appl. Mater. Interfaces **9**(44), 38863–38869 (2017).
[9] V. Dhinakaran, M. Lavanya, K. Vigneswari, M. Ravichandran, and M.D. Vijayakumar, "Review on exploration of graphene in diverse applications and its future horizon," Mater. Today Proc. **27**, 824–828 (2020).
[10] J. Dugay, M. Aarts, M. Giménez-Marqués, T. Kozlova, H.W. Zandbergen, E. Coronado, and H.S.J. van der Zant, "Phase Transitions in Spin-Crossover Thin Films Probed by Graphene Transport Measurements," Nano Lett. **17**(1), 186–193 (2017).
[11] E.P. Geest, K. Shakouri, W. Fu, V. Robert, V. Tudor, S. Bonnet, and G.F. Schneider, "Contactless Spin Switch Sensing by Chemo-Electric Gating of Graphene," Adv. Mater. **32**(10), 1903575 (2020).
[12] N. Konstantinov, A. Tauzin, U.N. Noumbé, D. Dragoe, B. Kundys, H. Majjad, A. Brosseau, M. Lenertz, A. Singh, S. Berciaud, M.-L. Boillot, B. Doudin, T. Mallah, and J.-F. Dayen, "Electrical read-out of light-induced spin transition in thin film spin crossover/graphene heterostructures," J. Mater. Chem. C **9**(8), 2712–2720 (2021).
[13] "Electrical Sensing of the Thermal and Light-Induced Spin Transition in Robust Contactless Spin-Crossover/Graphene Hybrid Devices - Gavara-Edo - 2022 - Advanced Materials - Wiley Online Library," (n.d.).
[14] J. Garcia-Amorós, A. Bučinskas, M. Reig, S. Nonell, and D. Velasco, "Fastest molecular photochromic switches based on nanosecond isomerizing benzothiazolium azophenolic salts," J Mater Chem C **2**(3), 474–480 (2014).
[15] J. Han, Z. Nelson, M.R. Chua, T.M. Swager, F. Niroui, J.H. Lang, and V. Bulović, "Molecular Platform for Fast Low-Voltage Nanoelectromechanical Switching," Nano Lett. **21**(24), 10244–10251 (2021).
[16] T.K. Ekanayaka, K.P. Maity, B. Doudin, and P.A. Dowben, "Dynamics of Spin Crossover Molecular Complexes," Nanomaterials **12**(10), 1742 (2022).
[17] L. Liao, and X. Duan, "Graphene for radio frequency electronics," Mater. Today **15**(7), 328–338 (2012).
[18] C. Yim, N. McEvoy, and G.S. Duesberg, "Characterization of graphene-silicon Schottky barrier diodes using impedance spectroscopy," Appl. Phys. Lett. **103**(19), 193106 (2013).
[19] P.M. Jordan, D.K. Simon, T. Mikolajick, and I. Dirnstorfer, "Trapped charge densities in Al_2O_3-based silicon surface passivation layers," J. Appl. Phys. **119**(21), 215306 (2016).

[20] B. Ki Min, S.K. Kim, S. Jun Kim, S. Ho Kim, M.-A. Kang, C.-Y. Park, W. Song, S. Myung, J. Lim, and K.-S. An, "Electrical Double Layer Capacitance in a Graphene-embedded Al2O3 Gate Dielectric," Sci. Rep. **5**(1), 16001 (2015).
[21] E.M. Mills, B.K. Min, S.K. Kim, S.J. Kim, M.-A. Kang, W. Song, S. Myung, J. Lim, K.-S. An, J. Jung, and S. Kim, "Direct Determination of Field Emission across the Heterojunctions in a ZnO/Graphene Thin-Film Barristor," ACS Appl. Mater. Interfaces **7**(33), 18300–18305 (2015).
[22] B.K. Min, S.K. Kim, S.H. Kim, M.-A. Kang, S. Noothongkaew, E.M. Mills, W. Song, S. Myung, J. Lim, S. Kim, and K.-S. An, "AC-Impedance Spectroscopic Analysis on the Charge Transport in CVD-Grown Graphene Devices with Chemically Modified Substrates," ACS Appl. Mater. Interfaces **8**(41), 27421–27425 (2016).
[23] M. Palluel, L.E. Khoury, N. Daro, S. Buffière, M. Josse, M. Marchivie, and G. Chastanet, "Rational direct synthesis of [Fe(Htrz)2(trz)](BF4) polymorphs: temperature and concentration effects," Inorg. Chem. Front. **8**(15), 3697–3706 (2021).
[24] J.-F. Dayen, N. Konstantinov, M. Palluel, N. Daro, B. Kundys, M. Soliman, G. Chastanet, and B. Doudin, "Room temperature optoelectronic devices operating with spin crossover nanoparticles," Mater. Horiz. **8**(8), 2310–2315 (2021).
[25] Y.D. Kim, M.-H. Bae, J.-T. Seo, Y.S. Kim, H. Kim, J.H. Lee, J.R. Ahn, S.W. Lee, S.-H. Chun, and Y.D. Park, "Focused-Laser-Enabled p–n Junctions in Graphene Field-Effect Transistors," ACS Nano **7**(7), 5850–5857 (2013).
[26] I. Lundström, and C. Svensson, "Tunneling to traps in insulators," J. Appl. Phys. **43**(12), 5045–5047 (1972).
[27] S. Peng, Z. Jin, Y. Yao, X. Huang, D. Zhang, J. Niu, J. Shi, Y. Zhang, and G. Yu, "Controllable p-to-n Type Conductance Transition in Top-Gated Graphene Field Effect Transistor by Interface Trap Engineering," Adv. Electron. Mater. **6**(9), 2000496 (2020).
[28] B. Karpiak, A. Dankert, and S.P. Dash, "Gate-tunable Hall sensors on large area CVD graphene protected by h-BN with 1D edge contacts," J. Appl. Phys. **122**(5), 054506 (2017).
[29] I. Amit, T.J. Octon, N.J. Townsend, F. Reale, C.D. Wright, C. Mattevi, M.F. Craciun, and S. Russo, "Role of Charge Traps in the Performance of Atomically Thin Transistors," Adv. Mater. **29**(19), 1605598 (2017).
[30] K.J. Sarkar, B. Pal, and P. Banerji, "Graphene Oxide as a Dielectric and Charge Trap Element in Pentacene-Based Organic Thin-Film Transistors for Nonvolatile Memory," ACS Omega **4**(2), 4312–4319 (2019).
[31] A. Bousseksou, G. Molnár, P. Demont, and J. Menegotto, "Observation of a thermal hysteresis loop in the dielectric constant of spin crossover complexes: towards molecular memory devices," J Mater Chem **13**(9), 2069–2071 (2003).
[32] H. Lee, K. Paeng, and I.S. Kim, "A review of doping modulation in graphene," Synth. Met. **244**, 36–47 (2018).
[33] A.K. Singh, R.S. Singh, and A.K. Singh, "Recent Developments in Chemical Doping of Graphene using Experimental Approaches and Its Applications," Adv. Eng. Mater. **24**(11), 2200259 (2022).
[34] Y. Hu, M. Picher, N.M. Tran, M. Palluel, L. Stoleriu, N. Daro, S. Mornet, C. Enachescu, E. Freysz, F. Banhart, and G. Chastanet, "Photo-Thermal Switching of Individual Plasmonically Activated Spin Crossover Nanoparticle Imaged by Ultrafast Transmission Electron Microscopy," Adv. Mater. **33**(52), 2105586 (2021).